water

MDPI

Article

Degradation of Atrazine by Flow-Through UV-Based Advanced Oxidation Processes: Roles of Light Source and Chlorine Addition

Suona Zhang [1], Tao Han [2], Li You [2], Jing Zhong [3], Huimin Zhang [3], Xiaojun Hu [1,*] and Wentao Li [2,4,*]

[1] School of Chemical and Environmental Engineering, Shanghai Institute of Technology, 100 Haiquan Road, Shanghai 201418, China
[2] State Key Laboratory of Environmental Aquatic Chemistry, Research Center for Eco-Environmental Sciences, Chinese Academy of Sciences, Beijing 100085, China
[3] Beijing Onyx Environmental Technology Co., Ltd., Beijing 100084, China
[4] School of Environmental Science and Engineering, Shanghai Jiao Tong University, Shanghai 200240, China
* Correspondence: hu-xj@sit.edu.cn (X.H.); wtli@rcees.ac.cn (W.L.)

Abstract: Understanding the degradation kinetics and mechanisms of trace organic contaminants (TrOCs) by UV-based advanced oxidation processes (UV-AOPs) are pivotal in realizing their efficient application in water treatment. However, the relevant knowledge in practical flow-through reactors remains a void, compared with that of commonly used batch reactors. To fill the knowledge gaps, the current work investigated the degradation of atrazine (ATZ) in flow-through UV-AOP systems with different light sources and chlorine additions. The results showed that UV/Cl_2 in the reactors (with a diameter of 50 mm) was not very efficient in ATZ degradation while the pseudo-first order degradation rate constant was elevated by over 2.7 times with vacuum UV (VUV)/UV. In contrast to observations in the batch reactors, the addition of chlorine to the flow-through VUV/UV system unexpectedly decreased the rate constant by about 39%. The analysis of the relative contributions of different degradation pathways revealed that the inhibitory effect of the chlorine addition arose from the transformation of $HO^{\bullet}$ to reactive chlorine species (e.g., $ClO^{\bullet}$) which had low reaction rate constants with ATZ. The baffle implementation promoted the ATZ degradation by 12–58%, mainly due to an enhanced mixing that facilitated the radical oxidation. The energy costs of the UV-AOPs in ATZ removal ranged within 0.40–1.11 kWh m^{-3} $order^{-1}$. The findings of this work are helpful in guiding efficient VUV/UV and VUV/UV/Cl_2 processes in drinking water treatment.

Keywords: water treatment; trace organic contaminant removal; advanced oxidation; flow-through reactor; VUV/UV; chlorine addition; inhibition effect

check for updates

Citation: Zhang, S.; Han, T.; You, L.; Zhong, J.; Zhang, H.; Hu, X.; Li, W. Degradation of Atrazine by Flow-Through UV-Based Advanced Oxidation Processes: Roles of Light Source and Chlorine Addition. *Water* **2024**, *16*, 1697. https://doi.org/10.3390/w16121697

Academic Editor: José Alberto Herrera-Melián

Received: 18 April 2024
Revised: 31 May 2024
Accepted: 8 June 2024
Published: 14 June 2024

Copyright: © 2024 by the authors. Licensee MDPI, Basel, Switzerland. This article is an open access article distributed under the terms and conditions of the Creative Commons Attribution (CC BY) license (https://creativecommons.org/licenses/by/4.0/).

1. Introduction

The occurrence of trace organic contaminants (TrOCs) such as pesticides, herbicides, industrial chemicals, pharmaceuticals, and personal care products in aquatic systems has been well documented in the past decades [1,2]. Taking atrazine as an example, a widely used and frequently detected herbicide, it finds its way into surface water with agricultural runoff and wastewater effluent, and eventually ends at concentrations of up to several μg/L [3,4]. The presence of these contaminants poses a great risk to aquatic organisms as well as human beings since they are recalcitrant, persistent in the environment, and toxic at concentrations in the low μg/L to ng/L range [2,5]. Conventional water treatment processes such as coagulation and sand filtration usually exhibit a limited effect on TrOCs removal [3,6–9]. To ensure a safe drinking water supply, advanced oxidation processes (AOPs) have been widely investigated and applied for the elimination of these contaminants [10–14]. Specifically, highly reactive species (e.g., $HO^{\bullet}$) generated with the introduction of chemicals (e.g., O_3, H_2O_2), high-energy radiation, or catalysts could vigorously destruct the TrOCs [11–14].

UV-based advanced oxidation processes (UV-AOPs, e.g., UV/H_2O_2 and UV/Cl_2) represent one of the most promising technologies for the abatement of TrOCs, where decontamination pathways of both direct photolysis and radical oxidation could be involved [5,11,15–18]. For instance, the widely acknowledged recalcitrant atrazine and carbamazepine could be efficiently degraded by UV/Cl_2, attributed mainly to the generated hydroxyl radicals ($HO^•$) and reactive chlorine species (RCS, including $Cl^•$, $Cl_2^{•-}$, and $ClO^•$) [19,20]. Among these studies, great efforts have been made in understanding the influential parameters such as the water matrix or oxidant dose in the respective UV-AOPs [18,19,21]. The presence of HCO_3^-/CO_3^{2-} was found to significantly inhibit the removal of contaminants in UV/Cl_2 systems, because the anions could transform primary radicals into less reactive carbonate radicals (Equations (1) and (2)) [13,15]. Recently, UV light sources emitting dual wavelengths, i.e., the 185 nm vacuum UV (VUV) and the 254 nm UV, have been employed to improve the UV/Cl_2 performance [22–24]. The benefit lies in that the 185 nm irradiation can be strongly adsorbed by water molecules, leading to additional generation of $HO^•$ (Equations (3) and (4)) [24,25]. A synergistic effect on TrOC removal has been reported with the combined VUV/UV/Cl_2 process, as compared to the sole VUV/UV and UV/Cl_2 process [18,23,26]. Nonetheless, most of these studies were conducted in batch reactors where the chemicals were well mixed. Taking into account the disparate flow patterns of batch and practical reactors (i.e., complete mixing vs. near-plug flow), the performances of UV-AOPs in practical flow-through reactors could deviate from those in batch reactors [17,27–29]. Clarifying the impact of reactor configuration (particularly the hydrodynamics) on process efficiency is fundamental to the implementation of UV-AOPs in real-world applications.

$$HO^• + HCO_3^- \rightarrow CO_3^{•-} + H_2O \quad (1)$$

$$Cl^• + HCO_3^- \rightarrow CO_3^{•-} + H^+ + Cl^- \quad (2)$$

$$H_2O \xrightarrow{h\upsilon_{185}} HO^• + H^• \quad (3)$$

$$H_2O \xrightarrow{h\upsilon_{185}} HO^• + e^- + H^+ \quad (4)$$

The configuration of a UV or VUV/UV reactor (e.g., reactor diameter and inner structure) could affect the radiation distribution and fluid flow in the reactor chamber. Due to divergence and absorption, the light intensity decreased with the increased distance from the center of the reactor where the lamp was installed [30,31]. In fact, the UV-induced atrazine degradation rate decreased with the increase in UV/Cl_2 reactor diameter, mainly due to the reduced average fluence rate [28]. The different flow patterns in reactors with diverse configurations would result in the varied utilization efficiency of the radicals and consequently contaminant degradation [29]. For instances, the implementation of baffles inside the VUV/UV reactor could promote *p*-chlorobenzoic acid degradation by 65% due to the optimization in hydrodynamics and a better interaction with radicals [27]. For the VUV/UV/Cl_2 process, the impact of reactor configuration is expected to be more complicated. The roles of the light source (i.e., VUV/UV vs. UV) and chlorine addition herein could differ from those in batch reactors, which has been rarely investigated.

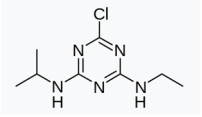
To fill these important knowledge gaps, the current work investigated the degradation kinetics and mechanisms of atrazine (ATZ), a model organic contaminant that is frequently detected in bothsource and finished drinking water, in flow-through UV, and in VUV/UV reactors. This is more representative of real-world application scenarios. The influence of conditions including light source and chlorine addition were systematically investigated in reactors with or without baffles. The relative contributions of UV photolysis, $HO^•$, and RCS oxidation in ATZ degradation were also analyzed. Finally, the energy costs of the different UV treatments were evaluated. The findings of this work are helpful in realizing efficient TrOC removal by UV-AOPs through the optimization of reactor configuration and operation conditions.

2. Materials and Methods

2.1. Chemicals

HPLC grade organic solvents including acetonitrile (ACN, >99.9%), methanol (MeOH, >99.9%), and formic acid (FA, >99.9%) were purchased from Fisher, Gosselies, Belgium. Sodium hypochlorite (NaClO, analytical grade, ≥95%) was obtained from Aladdin, Shanghai, China and the sodium sulfite (Na_2SO_3, analytical grade, ≥95%) was purchased from Sinochem, shanghai, China. Atrazine (ATZ, >97%) and nitrobenzene (NB, >97%) were supplied by TCI (Shanghai, China) and Sigma-Aldrich (St. Louis, MO, USA), respectively. Stock solutions of ATZ and NB were prepared with deionized water and stored at 4 °C before use. The structure and basic physicochemical properties of ATZ can be found in Table 1.

Table 1. The structure and basic physicochemical properties of ATZ.

Compound name	Atrazine
Chemical formula	C8H14ClN5
Molecular weight	215.68 g/mol
Solubility in water	34 mg/L at 25 °C
Log P (octanol-water partition coefficient)	2.63
pKa	1.68
Molecular structure	

2.2. Atrazine Degradation Experiments

The ATZ degradation experiments were conducted at room temperature (about 25 °C) in flow-through UV or VUV/UV reactors, as illustrated in Figure 1. Temperatures of both the influent and effluent were monitored, which fell within 23 ± 2 °C. The diameter of the reactors was the same at 50 mm, the height was 500 mm, and the volume of the chamber was 970 mL for the ordinary annular reactor (denoted as D50 reactor) and decreased to 887 mL when retrofitted with 5 ring baffles (width 7.5 mm) on the wall (denoted as the D50−5 reactor). The UV lamp (21 W, GCL436T5L; LightSources, Austin, TX, USA) was housed in a quartz sleeve and mounted at the center of the reactor. A UV-proof shield was applied to avoid the leakage of UV light into the environment while keeping away possible interference from ambient radiation. For the VUV/UV and VUV/UV/Cl_2 processes, a dual-wavelength UV lamp (21 W, GCL436T5VH/4; LightSources, Austin, TX, USA) was used where the portion of VUV irradiation was about 4%. The average UV fluence rate (at 254 nm) in the reactor chamber was about 12 mW cm^{-2} as measured using ATZ (2 μM) as the chemical actinometer [32]. Specifically, the actinometer solution was circulated between the influent tank and UV reactor (sole UV photolysis), and the degradation rate constant of ATZ was obtained by measuring residual concentration at preset time intervals, which correlated linearly with the average UV fluence rate. For experiments with the addition of chlorine, ATZ (2.5 μM or 0.54 mg L^{-1}) and chlorine (50 μM or 3.55 mg L^{-1}) were separately stored and then pumped into the reactor at designed flow rates to avoid their possible reaction (i.e., chlorination of ATZ) prior to exposure. The hydraulic retention time (HRT, 0–100 s) of the contaminant in the reactor was adjusted by changing the flow rate of the peristaltic pump. The samples were collected at the outlet of the reactor and immediately quenched with Na_2SO_3 to remove residual chlorine. The concentration of ATZ at different HRTs was determined using HPLC with the operating parameters listed in Table 2.

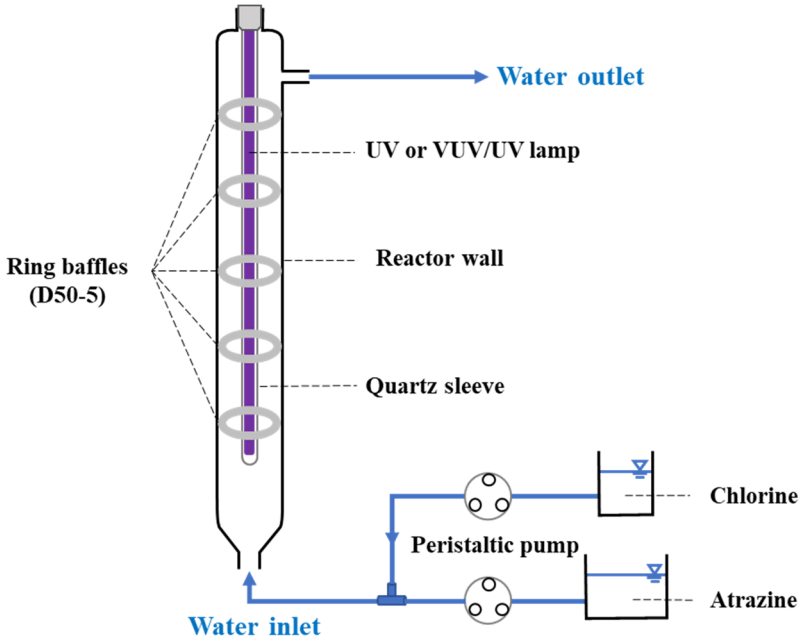


Figure 1. Schematic diagram of the flow-through UV or VUV/UV system. The D50 reactor had a diameter of 50 mm while the D50−5 reactor was further retrofitted with 5 ring baffles on the reactor wall.

Table 2. Detection parameters for HPLC analysis.

Analytes	Mobile Phase	Detection Wavelength (nm)	Injection Volume (μL)	Flow Rate (mL min^{-1})	Column Temperature (°C)
ATZ	ACN:0.2%FA = 75:25	234	50	0.8	40
NB	ACN:0.1%FA = 60:40	265	100	1.0	20

2.3. Determination of Relative Contributions of the Radicals

The ATZ in the flow could be degraded due to UV photolysis, chlorination, and radical oxidation. To understand the relative contributions of $HO^{\bullet}$ and RCS in the ATZ degradation, NB (2.0 μM, spiked together with ATZ) was used as a probe compound for the determination of the steady-state concentration of $HO^{\bullet}$ ($[HO^{\bullet}]_{ss}$) in the reaction system [11,33,34]. Specifically, NB could react with $HO^{\bullet}$ at a rate constant $k_{NB\times HO\bullet}$ of 3.9×10^9 M^{-1} s^{-1}, while its reaction with RCS including $Cl^{\bullet}$, $Cl_2^{\bullet-}$, and $ClO^{\bullet}$ was negligible [33,35]. By calculating the observed pseudo-first order rate constant of NB ($k_{obs,NB}$) which equaled the slope of the linear fitting curve of the logarithmic removal of NB with HRT (Equation (5)), the $[HO^{\bullet}]_{ss}$ could be quantified using Equation (6) [34]. Subsequently, the degradation rate constants of ATZ with $HO^{\bullet}$ ($k_{ATZ,HO\bullet}$) and RCS ($k_{ATZ,RCSs}$) were solved following Equations (7) and (8), respectively. The relative contribution of each pathway to ATZ removal was then determined by dividing the respective degradation rate constant (e.g., $k_{ATZ,HO\bullet}$) by the observed pseudo-first order rate constant (i.e., $k_{obs,ATZ}$).

$$k_{obs,\,NB} = \frac{-\ln([NB]/[NB]_0)}{HRT} \quad (5)$$

$$[HO^{\bullet}]_{ss} = \frac{k_{obs,\,NB}}{k_{NB\times HO^{\bullet}}} \quad (6)$$

$$k_{ATZ,\,HO^{\bullet}} = k_{ATZ\times HO^{\bullet}}[HO^{\bullet}]_{ss} \quad (7)$$

$$k_{ATZ,\,RCSs} = k_{obs,\,ATZ} - \left(k_{ATZ,\,HO^{\bullet}} + k_{ATZ,\,UV} + k_{ATZ,\,chlorination}\right) \quad (8)$$

where $k_{obs,NB}$ and $k_{obs,ATZ}$ are the observed pseudo-first order rate constants of NB and ATZ in the UV/Cl_2 or VUV/UV/Cl_2 system obtained as the slopes of the linear fitting curves, s^{-1}; $k_{ATZ,UV}$ and $k_{ATZ,chlorination}$ are the degradation rate constants of ATZ with sole UV photolysis and chlorination, s^{-1}, respectively; and $k_{ATZ\times HO^{\bullet}}$ is the second order rate constant of ATZ with $HO^{\bullet}$, which is 2.3×10^9 M^{-1} s^{-1}. It should be noted that the chlorination rate constant of ATZ (i.e., $k_{ATZ,chlorination}$) is approximately zero since ATZ degradation scarcely happens with only chlorine.

2.4. Evaluation of the E_{EO} of the UV-AOPs

The energy cost of UV-AOPs is usually evaluated with the electrical energy per order (E_{EO}, kWh m^{-3}), which is comprised here of the electrical energy arising from UV irradiation ($E_{EO\text{-}UV}$) and the equivalent electrical energy cost with chlorine addition ($E_{EO\text{-}Cl_2}$), and can be calculated as the following Equation (9) [16,28]:

$$E_{EO} = E_{EO\text{-}UV} + E_{EO\text{-}Cl_2} = \frac{1000 \times W_{UV}}{3600 \times 0.4343 V k_{obs,ATZ}} + Eq_{Cl_2} \times \frac{[Cl_2] \times 1000}{0.4343 k_{obs,ATZ} t} \quad (9)$$

where W_{UV} is the output power of the UV lamp, kW; V is the reactor volume, L; $k_{obs,ATZ}$ is the observed pseudo-first order rate constant of ATZ in the UV-AOP system, s^{-1}; Eq_{Cl2} represents the equivalent electrical energy consumption by dosing 1 mole of chlorine (provided by NaClO), which is determined to be 0.851 kWh mol^{-1} for the purchased lab reagent [16]; $[Cl_2]$ is the concentration of chlorine, M (or mol L^{-1}); and t is the HRT, s.

3. Results and Discussion

3.1. ATZ Degradation in Flow-Through UV-AOP Systems

The changes in ATZ concentration (i.e., expressed as $\ln(C/C_0)$) as a function of HRTs in the D50 and D50−5 reactors are shown in Figure 2. Generally, the ATZ degradation by different flow-through UV-AOPs followed pseudo-first order reaction kinetics where the rate constants ($k_{obs,ATZ}$) were reflected as the slopes of the linear fitting curves. The correlation coefficients of the fittings in the VUV/UV systems ($R^2 \geq 0.90$) were slightly smaller than those of the UV systems ($R^2 \geq 0.92$), indicating that the practical flow pattern (i.e., with a flow-through reactor) had a greater impact on the ATZ degradation by VUV/UV. The $k_{obs,ATZ}$ values of different UV treatments were compared in Figure 3. The ATZ degradation rate constant was 1.05×10^{-2} s^{-1} in the D50 reactor under UV photolysis, while it increased by 18% to 1.24×10^{-2} s^{-1} after chlorine addition (i.e., UV/Cl_2). In comparison, the rate constant increased from 5.38×10^{-3} s^{-1} of UV photolysis to 8.15×10^{-3} s^{-1} of UV/Cl_2 (by 51%) in the same reactor with a halved UV intensity [28]. The different extents of change in the $k_{obs,ATZ}$ with the addition of chlorine implied that ATZ degradation by direct photolysis was strongly correlated with the incident UV intensity; however, the degradation in the UV/Cl_2 system could also be affected by other factors such as the degree of mixing in the reactor, which is discussed below.

When the light source was upgraded to the VUV/UV lamp, the $k_{obs,ATZ}$ in the D50 reactor significantly increased to 3.32×10^{-2} s^{-1}, which was over 2.7 times those in the UV systems (Figure 3). This improvement could be attributed to vigorous $HO^{\bullet}$ production from 185 nm irradiation of water, where the $HO^{\bullet}$ concentration could be even higher than that in the UV/Cl_2 system [29,36]. Nonetheless, the $k_{obs,ATZ}$ decreased to 2.01×10^{-2} s^{-1} in the VUV/UV/Cl_2 system, a reduction of 39% as compared with that of the VUV/UV system. The result was completely unexpected as synergistic effects had been previously reported when combining chlorine with VUV/UV irradiation [18,23,25,26]. For instance, the degradation of six pesticides (including ATZ) in a batch VUV/UV reactor was promoted with the addition of chlorine [18]. The synergistic factors (SFs) as defined by Equation (10) were calculated to be in the range of 1.57–2.84, implying an enhancement of at least 57% as compared to the summation of individual removals. A similar synergism was also reported in the bench scale mini-fluidic VUV/UV/Cl_2 system [23]. Following Equation (10), the SF for the VUV/UV/Cl_2 process in the D50 reactor was calculated to be 0.57, which indicated

an obvious inhibition of ATZ degradation after chlorine addition. The decreased rate constant could be caused by the competition for the primary radicals by free chlorine (HOCl and OCl^-), which synchronously generated RCS such as $ClO^•$ (Equations (11)–(13)). Contrary to the fast reaction between ATZ and $HO^•$, the second order rate constants of ATZ with $ClO^•$ and $Cl_2^{•-}$ were reported to be much lower ($\leq 1.0 \times 10^7$ M^{-1} s^{-1}) [37,38]. Therefore, the $k_{obs,ATZ}$ in the case with the addition of chlorine was affected by the extents of primary radicals being transformed to $ClO^•$ and $Cl_2^{•-}$. In a flow-through VUV/UV reactor with a diameter of 50 mm, the limited mixing of the flow could be a drive to the scavenging of the primary radicals (e.g., $HO^•$) by free chlorine, which led to a disparate combined effect as compared to those found in batch reactors.

$$SF = \frac{k_{VUV/UV/chlorine}}{kVUV/UV + k_{UV/chlorine} - k_{UV}} \quad (10)$$

$$HO^• + HOCl/OCl^- \rightarrow ClO^• + H_2O/OH^- \quad (11)$$

$$Cl^• + HOCl/OCl^- \rightarrow ClO^• + HCl/Cl^- \quad (12)$$

$$Cl^• + Cl^- \rightleftarrows Cl_2^{•-} \quad (13)$$

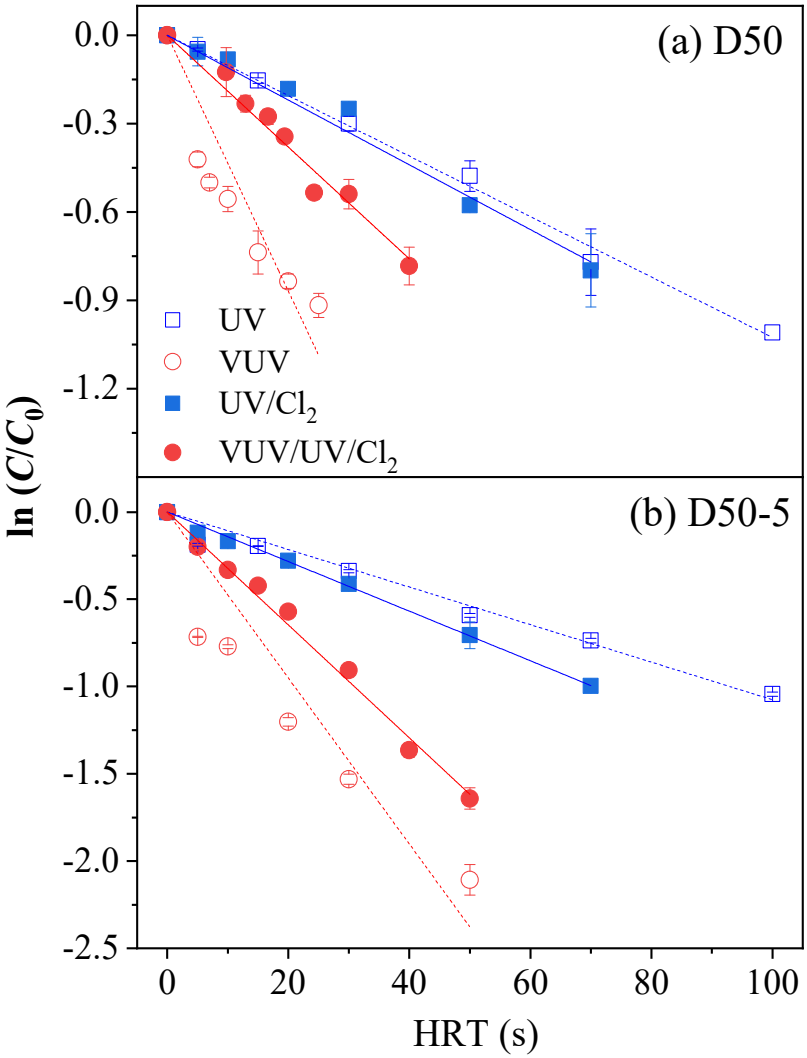


Figure 2. Degradation kinetics of ATZ by different UV treatments in the D50 and D50−5 reactors. Conditions: $[ATZ]_0$ = 2.5 μM, $[Cl_2]_0$ = 50 μM.

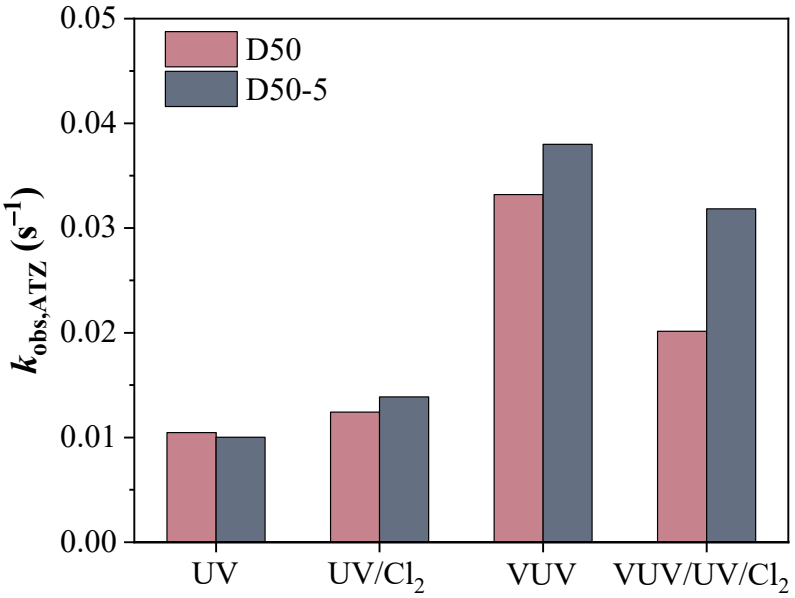


Figure 3. Pseudo first-order rate constants of ATZ degradation ($k_{obs,ATZ}$) by different UV treatments in the D50 and D50−5 reactors. Conditions: $[ATZ]_0$ = 2.5 μM, $[Cl_2]_0$ = 50 μM.

Similarly, for the D50−5 reactor, the ATZ degradation rate constant with the VUV/UV lamp increased to 3.80 × 10^{-2} s^{-1}, being 3.8- and 2.7-fold that of UV and UV/Cl_2 process, respectively. In addition, the $k_{obs,ATZ}$ for the VUV/UV/Cl_2 system (3.18 × 10^{-2} s^{-1}) was also smaller than that of VUV/UV system. As shown in Figure 3, the difference in ATZ degradation contributed by UV photolysis between the D50 and D50−5 reactors was very small. This reflected that the implementation of the ring baffles had a minor impact on the average fluence rate in the reactor chamber. However, the configuration modification resulted in a considerable change in ATZ degradation kinetics when radicals (either HO• or RCS) were involved in the system. Specifically, compared with that in the D50 reactor, the $k_{obs,ATZ}$ in the D50−5 reactor increased by 12%, 15%, and 58% for the VUV/UV, UV/Cl_2, and VUV/UV/Cl_2 processes, respectively. As discovered in previous studies, the diffusion rate of chemicals in flow-through reactors is low, especially when the flow is laminar (i.e., the Reynolds number < 2300) [36]. In the current work, the flow pattern varied from transient to laminar in the D50 reactor as the HRT increased (that is, the Reynolds number of the flow ranged from 700 to 4000). By implementing ring baffles in the reactor, mixing within the chamber was enhanced by the generated local vortices, which elevated the diffusion and utilization efficiency of radicals in the vicinity of the lamps [27]. The VUV/UV/Cl_2 process benefited the most from this configuration modification, mainly due to its largest concentration of radicals which would otherwise be quenched by free chlorine. In fact, the SF was calculated to be 0.76, a considerable elevation from 0.57 in the D50 reactor; however, there was still no synergistic effect. In summary, the chlorine addition inhibited the ATZ degradation in a flow-through VUV/UV reactor, and the reactor configuration had a significant impact on the extent of inhibition. It is advisable to perform specific inspections instead of relying simply on the findings of batch experiments before the application of a VUV/UV/Cl_2 process.

3.2. Relative Contributions of Different Degradation Pathways

The degradation of ATZ in VUV/UV/Cl_2 system is more complicated compared with the VUV/UV or UV/Cl_2 counterpart. This is because not only HO• and RCS could be generated upon VUV irradiation of the solution, chain reactions between the radicals and free chlorine would also occur. In addition, the reactor configuration could also exert an influence on the relative contributions of different degradation pathways. In general, the ATZ degradation could be induced by UV photolysis, HO•, and/or RCS oxidation. The

adsorption of VUV light by ATZ was negligible, considering the much higher adsorption coefficient (1.8 cm^{-1}) and molar concentration (55.6 M) of water [24]. As shown in Figure 4, the observed pseudo-first order rate constants of NB removal by VUV/UV/Cl_2 in the D50 and D50−5 reactors were 2.9 × 10^{-3} and 2.2 × 10^{-2} s^{-1}, respectively. Consequently, the steady-state concentrations of HO• ($[HO]_{ss}$) in the two reactors were calculated to be 0.74 × 10^{-12} and 5.6 × 10^{-12} M (Equation (6)). Following Equations (7) and (8), the relative contributions of HO• oxidation, RCS oxidation, and UV photolysis to ATZ degradation were determined and are presented in Figure 5.

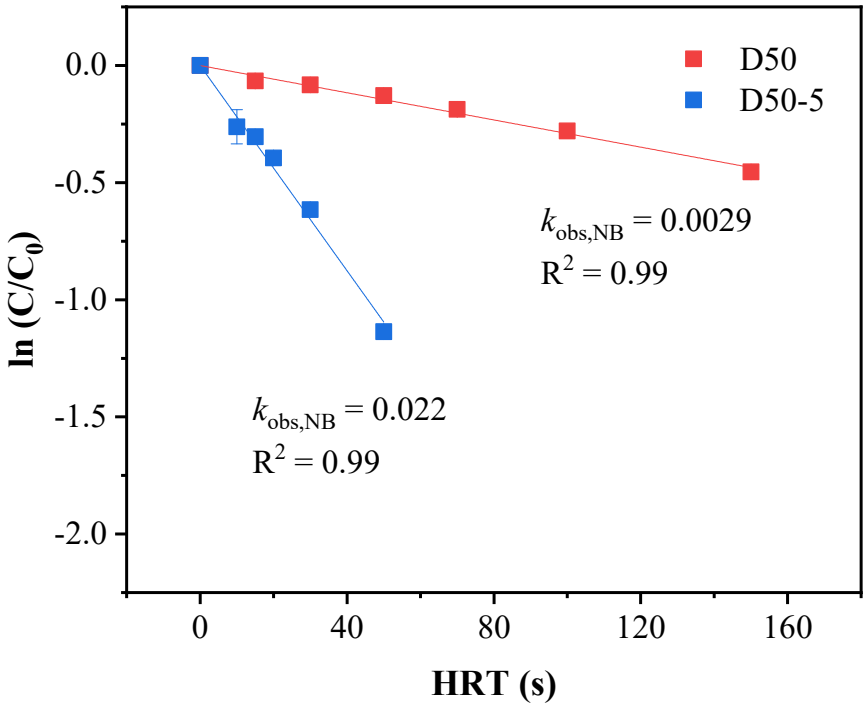


Figure 4. Degradation kinetics of NB by VUV/UV/Cl_2 in the D50 and D50−5 reactors. Conditions: $[NB]_0$ = 2.0 μM, $[Cl_2]_0$ = 50 μM.

For UV/Cl_2 in the D50 reactor, the relative contribution of UV photolysis to ATZ degradation was as large as 84% while that of RCS was only 3% (the left panel in Figure 5). This was completely different from that observed in a batch reactor where the radicals played the prime role (75%) in ATZ degradation [18]. The probable reasons included that the batch reactor had a larger diameter which facilitated UV photolysis of chlorine, and a complete mixing which elevated the radical utilization efficiency. Compared to the flow-through UV/Cl_2 system with a halved UV intensity [28], the enhanced ATZ degradation herein was caused primarily by the acceleration of UV photolysis. When the VUV/UV lamp was used (without chlorine addition), the dominant ATZ degradation pathway turned out to be that of HO• oxidation (i.e., 68%), arising from the intensive HO• generation through VUV photolysis of water. Nonetheless, the contribution of HO• oxidation decreased in the VUV/UV/Cl_2 system (i.e., 30%), largely due to the quenching of HO• through a competitive reaction with free chlorine (Equation (11)). In fact, the rate constant of ATZ degradation by HO• ($k_{ATZ,HO•}$) increased by over 10 times from 1.59 × 10^{-3} s^{-1} with UV/Cl_2 to 2.27 × 10^{-2} s^{-1} with VUV/UV, and then dropped to 6.07 × 10^{-3} s^{-1} in the VUV/UV/Cl_2 system. The relative contribution of the RCS was enhanced with the VUV/UV lamp (i.e., 18%) as more HO• were transformed to ClO•; however, due to its much lower reaction rate constant with ATZ (i.e., $k_{ATZ×ClO•} \leq 1.0 \times 10^7$ M^{-1} s^{-1}) [38], the $k_{obs,ATZ}$ in the VUV/UV/Cl_2 system was smaller than that of the VUV/UV (Figure 3). The relative contribution of UV photolysis remained as large as 31% in the flow-through

VUV/UV/Cl_2 system, much higher than that in the batch reactor [18], which was also due to the inhibited radical generation and utilization efficiency as mentioned above.

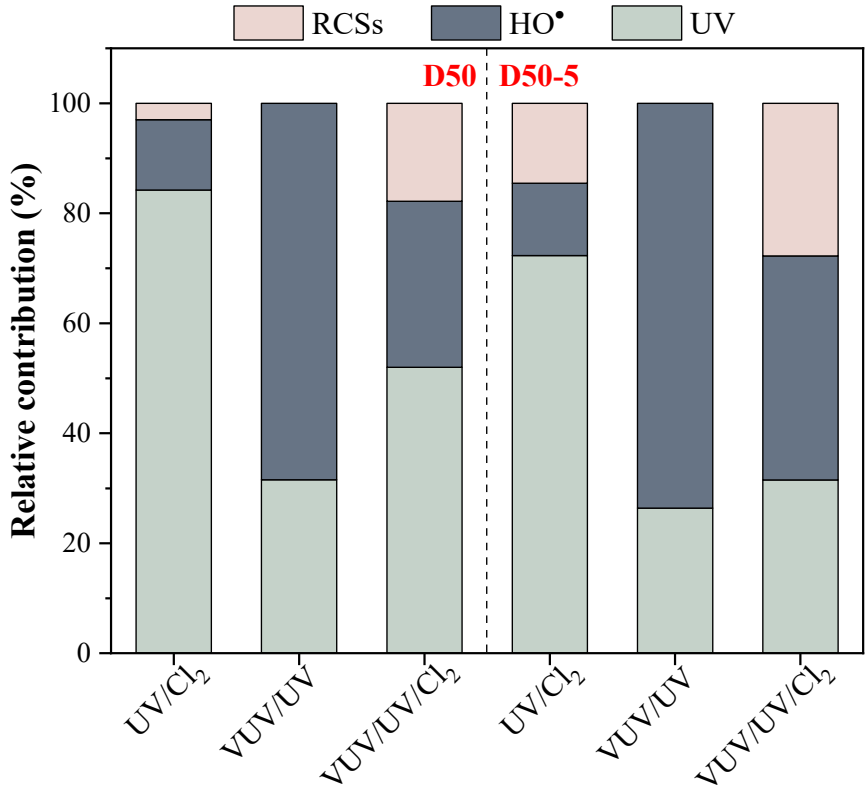


Figure 5. Relative contributions of UV photolysis, HO•, and RCS oxidation to ATZ degradation by UV/Cl_2, VUV/UV, and VUV/UV/Cl_2 in the D50 and D50−5 reactors. Conditions: $[ATZ]_0$ = 2.5 μM, $[Cl_2]_0$ = 50 μM.

In the D50−5 reactor (the right panel in Figure 5), the contributions of radical oxidation to ATZ degradation with the different UV-AOPs were all larger than those in the D50 reactor. Specifically, the relative contribution of the RCS was elevated to 15% in the UV/Cl_2 system, while that of HO• increased further to 74% with the VUV/UV. For the VUV/UV/Cl_2 system, contributions of both HO• and RCS were enhanced with the $k_{ATZ,HO•}$ and $k_{ATZ,RCS}$ being 1.30×10^{-2} s^{-1} and 8.83×10^{-3} s^{-1}, respectively, corresponding to relative contributions of 41% and 28%. The results confirmed the benefit of baffle implementation in improving the radical utilization efficiency. More efforts should be made to further optimize the flow-through VUV/UV/Cl_2 reactor for a potential synergistic effect as observed in batch reactors.

3.3. Evaluation of the Energy Cost

The E_{EO} values for ATZ degradation by UV photolysis in the D50 and D50−5 reactors were calculated to be 1.32 and 1.51 kWh m^{-3} $order^{-1}$, respectively, not economical for TrOC removal in drinking water [39]. With the addition of chlorine, the E_{EO} decreased to 1.11 and 1.09 kWh m^{-3} $order^{-1}$ in the two reactors (Figure 6). The reductions (i.e., 16% and 28%) were not as significant as expected, mainly due to the fact that the reactor diameter (i.e., 50 mm) was not favorable for the UV-driven process as a large portion of the UV light was absorbed by the reactor wall. Nonetheless, the radical-involved process was still promoted in the baffled reactor.

When the VUV/UV lamp was used, the E_{EO} for ATZ degradation in the D50 and D50−5 reactors decreased to 0.42 and 0.40 kWh m^{-3} $order^{-1}$, respectively. This was in accordance with the prominently increased degradation rate constants with the VUV/UV due to the large amount of HO• generated; meanwhile, the reactor diameter (i.e., 50 mm) was in a proper range for an efficient utilization of the radicals concentrated in the near-wall

region. For the VUV/UV/Cl_2 process, the respective E_{EO} values for ATZ degradation in the D50 and D50−5 reactors were 0.74 and 0.50 kWh m^{-3} $order^{-1}$, which were lower than those with UV/Cl_2 but higher than those for the VUV/UV process. These findings reflect that the combination of chlorine with VUV/UV irradiation would not necessarily decrease the energy cost, although the contribution of $E_{EO\text{-}Cl2}$ stayed relatively low (i.e., ≤7%) (Figure 6). In contrast, the adoption of an optimal reactor configuration (i.e., a proper reactor diameter and baffle implementation) was more crucial to the flow-through VUV/UV process. The advantage of a VUV/UV light source persisted in different reactors, with or without chlorine addition. Regarding real-world applications, for small-scale drinking water treatment (e.g., water supply in rural areas), the application of the VUV/UV lamp together with a small UV reactor was recommended for the degradation of the TrOCs such as ATZ [29]. However, for the treatment of drinking water and reclaimed water on a large scale, the application of the UV/Cl_2 process was suggested, where the E_{EO} could be further reduced by properly increasing the reactor diameter or oxidant dose.

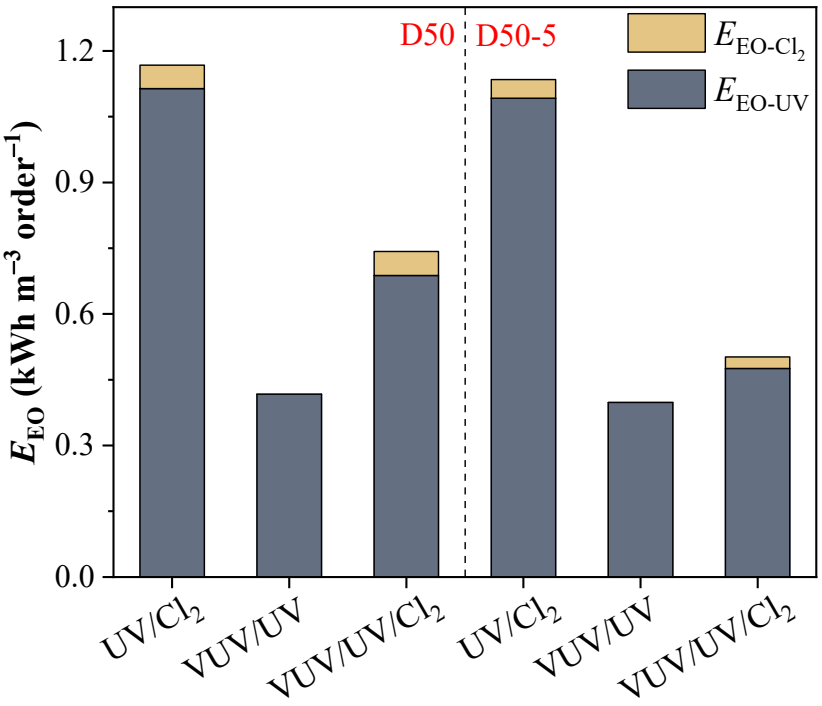


Figure 6. E_{EO} values of ATZ degradation by UV/Cl_2, VUV/UV, and VUV/UV/Cl_2 in the D50 and D50−5 reactors. Conditions: $[ATZ]_0$ = 2.5 μM, $[Cl_2]_0$ = 50 μM.

4. Conclusions

This work investigated the degradation of ATZ by UV-AOPs with a UV or VUV/UV light source in the less frequently studied flow-through reactors (i.e., compared with batch counterparts) with different reactor configurations. The role of the addition of chlorine was further explored by examining the changes in ATZ degradation kinetics and mechanisms, which were found to have significantly deviated from those observed with batch reactors. The energy costs of the different UV-AOPs were assessed with E_{EO}. The main findings are summarized as follows.

- The degradation of ATZ by UV, UV/Cl_2, VUV/UV, and VUV/UV/Cl_2 in the flow-through reactors followed the pseudo-first order reaction kinetics in general ($R^2 \geq 0.90$). The shift of light source from UV to VUV/UV significantly enhanced ATZ degradation. The $k_{obs,ATZ}$ with UV/Cl_2 was just slightly larger than that with UV photolysis due to an unfavorable small reactor diameter, while the addition of chlorine to VUV/UV process decreased significantly the rate constant (e.g., from 3.32×10^{-2} to 2.01×10^{-2} s^{-1}

in the D50 reactor). The implementation of baffles elevated the $k_{obs,ATZ}$ with the different UV-AOPs by 12–58%.

- UV photolysis contributed primarily (as large as 84%) to the ATZ degradation, while $HO^{\bullet}$ oxidation dominated the ATZ degradation by VUV/UV ($\geq$68%). The relative contribution of $HO^{\bullet}$ oxidation dropped to as low as 30% in the VUV/UV/Cl_2 process while that of RCS increased to 18%. This indicated a considerable transformation of $HO^{\bullet}$ to the less reactive RCS by free chlorine, which explained the inhibition role of the chlorine addition to the flow-through VUV/UV process. The baffle implementation could somewhat alleviate the inhibition effect.
- The E_{EO} values ranged from 0.42 to 1.11 and 0.40 to 1.09 kWh m^{-3} $order^{-1}$ in the D50 and D50−5 reactors, respectively. The lowest E_{EO} was consistently identified with the VUV/UV process and the baffled reactor had a slight advantage over the annular reactor. Collectively, the VUV/UV process in reactors with a proper diameter and baffle allocation is promising for ATZ removal in small-scale water treatments.

Author Contributions: S.Z.: conceptualization, data curation, writing—original draft, and writing—review and editing; T.H.: methodology, formal analysis, investigation, data acquisition, and writing—original draft; L.Y.: investigation, data acquisition, and validation; J.Z.: methodology, investigation, and resources; H.Z.: methodology and investigation; X.H.: conceptualization, funding acquisition, supervision, and writing—review and editing; W.L.: conceptualization, funding acquisition, supervision, and writing—review and editing. All authors have read and agreed to the published version of the manuscript.

Funding: This research was funded by National Natural Science Foundation of China grant number 51908536, the Beijing Municipal Natural Science Foundation grant number 8212037 and the Natural Science Foundation of Shanghai grant number 23ZR1462300.

Data Availability Statement: Data is contained within the article.

Conflicts of Interest: Authors Jing Zhong and Huimin Zhang were employed by the company Beijing Onyx Environmental Technology Co., Ltd., Beijing, China. The remaining authors declare that the research was conducted in the absence of any commercial or financial relationships that could be construed as a potential conflict of interest.

References

1. Stackelberg, P.E.; Furlong, E.T.; Meyer, M.T.; Zaugg, S.D.; Henderson, A.K.; Reissman, D.B. Persistence of pharmaceutical compounds and other organic wastewater contaminants in a conventional drinking-water-treatment plant. *Sci. Total Environ.* **2004**, *329*, 99–113. [CrossRef]
2. Bieber, S.; Snyder, S.A.; Dagnino, S.; Rauch-Williams, T.; Drewes, J.E. Management strategies for trace organic chemicals in water—A review of international approaches. *Chemosphere* **2018**, *195*, 410–426. [CrossRef]
3. Benotti, M.J.; Trenholm, R.A.; Vanderford, B.J.; Holady, J.C.; Stanford, B.D.; Snyder, S.A. Pharmaceuticals and endocrine disrupting compounds in US drinking water. *Environ. Sci. Technol.* **2009**, *43*, 597–603. [CrossRef]
4. Sousa, J.C.G.; Ribeiro, A.R.; Barbosa, M.O.; Pereira, M.F.R.; Silva, A.M.T. A review on environmental monitoring of water organic pollutants identified by EU guidelines. *J. Hazard. Mater.* **2018**, *344*, 146–162. [CrossRef]
5. Pisarenko, A.N.; Stanford, B.D.; Yan, D.; Gerrity, D.; Snyder, S.A. Effects of ozone and ozone/peroxide on trace organic contaminants and NDMA in drinking water and water reuse applications. *Water Res.* **2012**, *46*, 316–326. [CrossRef]
6. Vieno, N.M.; Härkki, H.; Tuhkanen, T.; Kronberg, L. Occurrence of pharmaceuticals in river water and their elimination in a pilot-scale drinking water treatment plant. *Environ. Sci. Technol.* **2007**, *41*, 5077–5084. [CrossRef]
7. Inyang, M.; Dickenson, E. The potential role of biochar in the removal of organic and microbial contaminants from potable and reuse water: A review. *Chemosphere* **2015**, *134*, 232–240. [CrossRef]
8. Eschauzier, C.; Beerendonk, E.; Scholte-Veenendaal, P.; De Voogt, P. Impact of treatment processes on the removal of perfluoroalkyl acids from the drinking water production chain. *Environ. Sci. Technol.* **2012**, *46*, 1708–1715. [CrossRef] [PubMed]
9. Reemtsma, T.; Berger, U.; Arp, H.P.H.; Gallard, H.; Knepper, T.P.; Neumann, M.; Quintana, J.B.; Voogt, P.d. Mind the Gap: Persistent and Mobile Organic Compounds—Water Contaminants That Slip Through. *Environ. Sci. Technol.* **2016**, *50*, 10308–10315. [CrossRef] [PubMed]
10. Liu, Z.; Demeestere, K.; Hulle, S.V. Comparison and performance assessment of ozone-based AOPs in view of trace organic contaminants abatement in water and wastewater: A review. *J. Environ. Chem. Eng.* **2021**, *9*, 105599. [CrossRef]
11. Fang, J.; Fu, Y.; Shang, C. The roles of reactive species in micropollutant degradation in the UV/free chlorine system. *Environ. Sci. Technol.* **2014**, *48*, 1859–1868. [CrossRef] [PubMed]

12. Beltrán, F.J.; Ovejero, G.; Acedo, B. Oxidation of atrazine in water by ultraviolet radiation combined with hydrogen peroxide. *Water Res.* **1993**, *27*, 1013–1021. [CrossRef]
13. von Gunten, U. Oxidation Processes in Water Treatment: Are We on Track? *Environ. Sci. Technol.* **2018**, *52*, 5062–5075. [CrossRef] [PubMed]
14. Eghbali, P.; Hassani, A.; Wacławek, S.; Andrew Lin, K.-Y.; Sayyar, Z.; Ghanbari, F. Recent advances in design and engineering of MXene-based catalysts for photocatalysis and persulfate-based advanced oxidation processes: A state-of-the-art review. *Chem. Eng. J.* **2024**, *480*, 147920. [CrossRef]
15. Choi, H.-J.; Kim, D.; Lee, T.-J. Photochemical degradation of atrazine in UV and UV/H_2O_2 process: Pathways and toxic effects of products. *J. Environ. Sci. Health Part B* **2013**, *48*, 927–934. [CrossRef] [PubMed]
16. Guo, K.; Wu, Z.; Yan, S.; Yao, B.; Song, W.; Hua, Z.; Zhang, X.; Kong, X.; Li, X.; Fang, J. Comparison of the UV/chlorine and UV/H_2O_2 processes in the degradation of PPCPs in simulated drinking water and wastewater: Kinetics, radical mechanism and energy requirements. *Water Res.* **2018**, *147*, 184–194. [CrossRef] [PubMed]
17. Xie, P.; Yue, S.; Ding, J.; Wan, Y.; Li, X.; Ma, J.; Wang, Z. Degradation of organic pollutants by Vacuum-Ultraviolet (VUV): Kinetic model and efficiency. *Water Res.* **2018**, *133*, 69–78. [CrossRef] [PubMed]
18. Yang, L.; Zhang, Z. Degradation of six typical pesticides in water by VUV/UV/chlorine process: Evaluation of the synergistic effect. *Water Res.* **2019**, *161*, 439–447. [CrossRef]
19. Wang, W.-L.; Wu, Q.-Y.; Huang, N.; Wang, T.; Hu, H.-Y. Synergistic effect between UV and chlorine (UV/chlorine) on the degradation of carbamazepine: Influence factors and radical species. *Water Res.* **2016**, *98*, 190–198. [CrossRef]
20. Sun, J.; Kong, D.; Aghdam, E.; Fang, J.; Wu, Q.; Liu, J.; Du, Y.; Yang, X.; Shang, C. The influence of the UV/chlorine advanced oxidation of natural organic matter for micropollutant degradation on the formation of DBPs and toxicity during post-chlorination. *Chem. Eng. J.* **2019**, *373*, 870–879. [CrossRef]
21. Chaves, F.P.; Gomes, G.; Della-Flora, A.; Dallegrave, A.; Sirtori, C.; Saggioro, E.M.; Bila, D.M. Comparative endocrine disrupting compound removal from real wastewater by UV/Cl and UV/H_2O_2: Effect of pH, estrogenic activity, transformation products and toxicity. *Sci. Total Environ.* **2020**, *746*, 141041. [CrossRef] [PubMed]
22. Du, J.; Liu, D.; Zhang, Z.; Ai, H.; Fu, M.-L.; Sun, W.; Yuan, B. Comparative effectiveness of sequential and synergistic (VUV/)UV and chlorine disinfection on DBPs and humic acid reduction. *Sep. Purif. Technol.* **2024**, *335*, 126083. [CrossRef]
23. Li, M.; Qiang, Z.; Hou, P.; Bolton, J.R.; Qu, J.; Li, P.; Wang, C. VUV/UV/Chlorine as an Enhanced Advanced Oxidation Process for Organic Pollutant Removal from Water: Assessment with a Novel Mini-Fluidic VUV/UV Photoreaction System (MVPS). *Environ. Sci. Technol.* **2016**, *50*, 5849–5856. [CrossRef] [PubMed]
24. Zoschke, K.; Börnick, H.; Worch, E. Vacuum-UV radiation at 185 nm in water treatment—A review. *Water Res.* **2014**, *52*, 131–145. [CrossRef] [PubMed]
25. Zhang, Y.-L.; Wang, W.-L.; Lee, M.-Y.; Yang, Z.-W.; Wu, Q.-Y.; Huang, N.; Hu, H.-Y. Promotive effects of vacuum-UV/UV (185/254 nm) light on elimination of recalcitrant trace organic contaminants by UV-AOPs during wastewater treatment and reclamation: A review. *Sci. Total Environ.* **2022**, *818*, 151776. [CrossRef] [PubMed]
26. Xiao, Z.-Y.; Huang, N.; Wang, Q.; Wang, W.-L.; Wu, Q.-Y.; Hu, H.-Y. Advanced oxidation of dodecyl dimethyl benzyl ammonium chloride by VUV/UV/chlorine: Synergistic effect, radicals, and degradation pathway. *Sep. Purif. Technol.* **2022**, *292*, 121012. [CrossRef]
27. Bagheri, M.; Mohseni, M. Impact of hydrodynamics on pollutant degradation and energy efficiency of VUV/UV and H_2O_2/UV oxidation processes. *J. Environ. Manag.* **2015**, *164*, 114–120. [CrossRef]
28. Han, T.; Li, W.; Li, J.; Jia, L.; Wang, H.; Qiang, Z. Degradation of micropollutants in flow-through UV/chlorine reactors: Kinetics, mechanism, energy requirement and toxicity evaluation. *Chemosphere* **2022**, *307*, 135890. [CrossRef] [PubMed]
29. Jia, L.; Chen, R.; Sun, Z.; Li, W.; Wang, H.; Qiang, Z. Degradation of micropollutants in flow-through VUV/UV reactors: Impact of internal diameter and baffle allocation. *Chemosphere* **2023**, *335*, 139112. [CrossRef]
30. Wols, B.; Hofman-Caris, C. Modelling micropollutant degradation in UV/H_2O_2 systems: Lagrangian versus Eulerian method. *Chem. Eng. J.* **2012**, *210*, 289–297. [CrossRef]
31. Li, W.; Li, M.; Wang, H.; Qiang, Z. Impact of Reactor Configuration on the Performance of UV/Persulfate Process for Atrazine Removal in Water: A CFD Modeling. *ACS ES&T Eng.* **2024**, *4*, 861–869. [CrossRef]
32. Canonica, S.; Meunier, L.; von Gunten, U. Phototransformation of selected pharmaceuticals during UV treatment of drinking water. *Water Res.* **2008**, *42*, 121–128. [CrossRef] [PubMed]
33. Watts, M.J.; Linden, K.G. Chlorine photolysis and subsequent OH radical production during UV treatment of chlorinated water. *Water Res.* **2007**, *41*, 2871–2878. [CrossRef] [PubMed]
34. Xiang, Y.; Fang, J.; Shang, C. Kinetics and pathways of ibuprofen degradation by the UV/chlorine advanced oxidation process. *Water Res.* **2016**, *90*, 301–308. [CrossRef] [PubMed]
35. Buxton, G.V.; Greenstock, C.L.; Helman, W.P.; Ross, A.B. Critical Review of rate constants for reactions of hydrated electrons, hydrogen atoms and hydroxyl radicals (·OH/·O^-) in Aqueous Solution. *J. Phys. Chem. Ref. Data* **1988**, *17*, 513–886. [CrossRef]
36. Bagheri, M.; Mohseni, M. Computational fluid dynamics (CFD) modeling of VUV/UV photoreactors for water treatment. *Chem. Eng. J.* **2014**, *256*, 51–60. [CrossRef]
37. Wojnárovits, L.; Takács, E. Rate constants of dichloride radical anion reactions with molecules of environmental interest in aqueous solution: A review. *Environ. Sci. Pollut. Res.* **2021**, *28*, 41552–41575. [CrossRef] [PubMed]

38. Wojnárovits, L.; Takács, E. Rate constants for the reactions of chloride monoxide radical ($ClO^{\bullet}$) and organic molecules of environmental interest. *Water Sci. Technol.* **2023**, *87*, 1925–1944. [CrossRef]
39. Miklos, D.B.; Remy, C.; Jekel, M.; Linden, K.G.; Drewes, J.E.; Hübner, U. Evaluation of advanced oxidation processes for water and wastewater treatment—A critical review. *Water Res.* **2018**, *139*, 118–131. [CrossRef]

Disclaimer/Publisher's Note: The statements, opinions and data contained in all publications are solely those of the individual author(s) and contributor(s) and not of MDPI and/or the editor(s). MDPI and/or the editor(s) disclaim responsibility for any injury to people or property resulting from any ideas, methods, instructions or products referred to in the content.